

Pex19p Interacts with Pex3p and Pex10p and Is Essential for Peroxisome Biogenesis in *Pichia pastoris*

William B. Snyder,^{*†} Klaas Nico Faber,^{*†‡} Thibaut J. Wenzel,^{*†}
Antonius Koller,^{*} Georg H. Lüers,^{*‡} Linda Rangell,[§] Gilbert A. Keller,[§]
and Suresh Subramani^{*||}

^{*}Department of Biology, University of California, San Diego, La Jolla, California 92093-0322; and

[§]Laboratory of Electron Microscopy, Genentech, South San Francisco, California 94080

Submitted February 5, 1999; Accepted March 15, 1999

Monitoring Editor: Chris Kaiser

We report the cloning and characterization of *Pichia pastoris* PEX19 by complementation of a peroxisome-deficient mutant strain. Import of peroxisomal targeting signal 1- and 2-containing peroxisomal matrix proteins is defective in *pex19* mutants. PEX19 encodes a hydrophilic 299-amino acid protein with sequence similarity to *Saccharomyces cerevisiae* Pex19p and human and Chinese hamster PxF, all farnesylated proteins, as well as hypothetical proteins from *Caenorhabditis elegans* and *Schizosaccharomyces pombe*. The farnesylation consensus is conserved in PpPex19p but dispensable for function and appears unmodified under the conditions tested. Pex19p localizes predominantly to the cytosolic fraction. Biochemical and two-hybrid analyses confirmed that Pex19p interacts with Pex3p, as seen in *S. cerevisiae*, but unexpectedly also with Pex10p. Two-hybrid analysis demonstrated that the amino-terminal 42 amino acids of Pex19p interact with the carboxyl-terminal 335 amino acids of Pex3p. In addition, the extreme carboxyl terminus of Pex19p (67 amino acids) is required for interaction with the amino-terminal 380 amino acids of Pex10p. Biochemical and immunofluorescence microscopy analyses of *pex19Δ* cells identified the membrane protein Pex3p in peroxisome remnants that were not previously observed in *S. cerevisiae*. These small vesicular and tubular (early) remnants are morphologically distinct from other *Pppex* mutant (late) remnants, suggesting that Pex19p functions at an early stage of peroxisome biogenesis.

INTRODUCTION

Peroxisomes are single-membrane-bound organelles found in virtually all eukaryotes (De Duve, 1996). Although their involvement in H₂O₂ metabolism is a general feature, specific metabolic functions vary depending on the organism and the milieu it encounters.

[†] These authors contributed equally.

[‡] Present addresses: (K.N.F.) University of Groningen, Department of Microbiology, 9751 NN Haren, The Netherlands; (T.J.W.) Gist-Brocades, Food Specialities Division, 2600 MA Delft, The Netherlands; (G.H.L.) University of Bonn, Institute for Anatomy, 53115 Bonn, Germany.

^{||} Corresponding author: E-mail address: ssubramani@ucsd.edu. Abbreviations used: ER, endoplasmic reticulum; GFP, green fluorescent protein; PMP, peroxisomal membrane protein; PNS, postnuclear supernatant; PTS, peroxisomal targeting signal; TCA, trichloroacetic acid.

β -oxidation (Lazarow and De Duve, 1976; Tolbert and Essner, 1981), plasmalogen biosynthesis (Hajra and Bishop, 1982), and cholesterol biosynthesis (Thompson and Krisans, 1990) are among the various activities residing in mammalian peroxisomes. The importance of these organelles in humans is stressed by the existence of a number of fatal genetic disorders in which the peroxisome is defective (Subramani, 1997). In cells of these patients, remnants containing peroxisomal membrane proteins (PMPs) are present, whereas some, or even all, peroxisomal matrix proteins accumulate in the cytosol (Lazarow and Moser, 1989).

In recent years, much progress has been made in elucidating the molecular requirements for peroxisome biogenesis, especially through the use of yeasts as model organisms. In *Pichia pastoris*, peroxisomes are

required for metabolizing carbon sources such as methanol and oleate but are dispensable for growth on glucose, glycerol, and ethanol. This feature made it relatively easy to obtain yeast mutants defective in peroxisome biogenesis. These mutants, and those in other yeasts, have contributed to the cloning and characterization of at least 21 *PEX* genes, encoding peroxins that are essential for peroxisome biogenesis (Distel *et al.*, 1996; Götte *et al.*, 1998; Purdue *et al.*, 1998; Subramani, 1998; Titorenko *et al.*, 1998). Screening the human Expressed Sequence Tags databases has revealed 13 human orthologues to the yeast *PEX* genes (Subramani, 1997; Fransen *et al.*, 1998). Eight of these genes have been shown to complement the peroxisome-related defects of cells from human disease complementation groups (Subramani, 1997). Clearly, peroxisome biogenesis is a conserved process in eukaryotes, and yeasts are preeminently suited to study this process at the molecular level.

Despite the growing number of *PEX* genes, few details are known about their individual functions. Eight peroxins, Pex5p, Pex7p, Pex13p, Pex14p, Pex17p, Pex18p, Pex20p, and Pex21p, have been primarily implicated in the process of peroxisomal matrix protein import (Purdue *et al.*, 1998; Subramani, 1998; Titorenko *et al.*, 1998). Peroxisomal matrix proteins are synthesized in the cytosol and posttranslationally imported into the organelle (Lazarow and Fujiki, 1985). Two peroxisomal targeting signals (PTSs) have been identified; PTS1, a carboxyl-terminal tripeptide (SKL and conserved derivatives) (Gould *et al.*, 1987, 1989; Elgersma *et al.*, 1996), is most commonly found in matrix proteins; PTS2, an amino-terminal nonapeptide (Osumi *et al.*, 1991; Swinkels *et al.*, 1991), is found in a smaller subset of proteins. Pex5p and Pex7p are the receptors for PTS1 and PTS2, respectively (Rehling *et al.*, 1996; Subramani, 1998). Three peroxisomal membrane-bound proteins, Pex13p, Pex14p, and Pex17p, interact to form a docking site on the organelle for these predominantly cytosolic signal receptors (Huhse *et al.*, 1998; Subramani, 1998). The mechanism of protein translocation across the peroxisome membrane, however, is essentially unknown.

Most of the peroxins characterized to date are PMPs. Information about the sorting of this class of proteins is only rudimentary. A sequence involved in sorting of PMPs has been identified for a few proteins. The presence of a stretch of basic amino acids (four in a sequence of six) is the most common feature of these sequences (Elgersma *et al.*, 1997). Although many PMPs seem to be synthesized in the cytosol and imported directly to the peroxisome, some were recently proposed to be targeted to the peroxisome via the endoplasmic reticulum (ER) (Titorenko and Rachubinski, 1998). This implies that a sorting machinery exists between the ER and the peroxisome, which was not envisioned in the original "multiplication-via-division

Table 1. *P. pastoris* strain list

Strain	Relevant genotype	Source
PPY12	<i>his4, arg4</i>	Gould <i>et al.</i> , 1992
SMD1163	<i>his4 pep4 prb</i>	Invitrogen
STW3	PPY12 pTW2	This study
STW4	<i>his4 arg4 pex19-112</i>	This study
SKF13	PPY12 <i>pex19Δ1::ZEO</i>	This study
SKF14	SMD1163 <i>pex19Δ1::ZEO</i>	This study
STW2	PPY12 <i>his4::pTW66</i>	Wiemer <i>et al.</i> , 1996
AK11	SKF13 <i>his4::pTW66</i>	This study
WSP50	SKF14 <i>his4::pWSP50</i>	This study
WSP51	SKF14 <i>his4::pWSP51</i>	This study
WSP52	SKF14 <i>his4::pWSP52</i>	This study
SSH4	SMD1163 <i>pex10Δ1::ZEO</i>	This study
SSH18	SSH4 <i>his4::pSH38</i>	This study
PPY12Δ2	PPY12 <i>pex2Δ::ARG4</i>	Jim Cregg
PPY12Δ5	PPY12 <i>pex5Δ::ARG4</i>	McCollum <i>et al.</i> , 1993

model" for peroxisome biogenesis (Lazarow and Fujiki, 1985).

Here we report the cloning of the *PEX19* gene and characterization of the gene product in *P. pastoris*. Previously, *PEX19* has been cloned and characterized from *Saccharomyces cerevisiae* (Götte *et al.*, 1998), Chinese hamster (PxF) (James *et al.*, 1994), and human cells (HK33/PxF) (Braun *et al.*, 1994; Kammerer *et al.*, 1997) and shown to be modified by farnesylation, but no evidence for this modification was seen in *P. pastoris*. Consistent between *S. cerevisiae* and *P. pastoris* is the accumulation of luminal peroxisomal proteins in the cytosol of *pex19* mutants, an effect that has not been observed in mammalian cells because of lack of *PEX19*-defective cell lines. Biochemical localization of Pex19p/PxF in all organisms has suggested that it is mainly cytosolic, but immunocytochemical evidence suggests that it associates with the peroxisome membrane (James *et al.*, 1994; Kammerer *et al.*, 1997; Götte *et al.*, 1998). Our results confirm a previously reported protein-protein interaction with Pex3p and also identify a novel one with Pex10p. In *S. cerevisiae*, no peroxisome remnant structures were observed in the *pex19* mutants (Götte *et al.*, 1998), but we present evidence that novel, morphologically distinct remnants are present in *P. pastoris*. The combination of novel cell biological, biochemical, and protein-protein interaction data allows us to augment models of Pex19p function beyond those reported previously.

MATERIALS AND METHODS

Strains and Growth Conditions

Strains used in this study are listed in Table 1 and were grown at 30°C. *P. pastoris* was grown in rich medium (YPD; 1% yeast extract, 2% Bacto-peptone, and 2% glucose) or synthetic medium (0.67% yeast nitrogen base) supplemented with 2% glucose (YND) or 0.5% (vol/vol) methanol (YNM). If needed, media were supplemented with appropriate amino acids to a final concentration of 50 μg/ml.

Table 2. Plasmids used in this study

Name	Relevant elements	Reference
pTW2	P _{AOX1} BLE-PTS1 <i>Sc</i> ARG4 PARS2	This study
pTW66	P _{GAPDH} PTS2-GFP <i>HIS4</i>	Wiemer <i>et al.</i> , 1996
p112Sal	pSG560 2.2 kb- <i>SalI</i> -PEX19	This study
pTW121	pSG560 1.4 kb PCR PEX19	This study
pKNSD169	<i>pex19Δ1::ZEO</i>	This study
pTW128	pQE9 <i>HIS₆-PEX19</i>	This study
pWSP50	pIB1 <i>PEX19 HIS4</i>	This study
pWSP51	pIB1 <i>pex19C296S HIS4</i>	This study
pWSP52	pIB1 <i>pex19C296ter HIS4</i>	This study
pSH5	<i>pex10Δ1::ZEO</i>	This study
pSH38	p21-43 <i>NH-PEX10</i>	This study
Two-hybrid plasmids		
pKNSD123	pKNSD52 <i>PEX19</i>	This study
pKNSD124	pKNSD55 <i>PEX19</i>	This study
pKNSD127	pKNSD52 <i>PEX19</i> [1-232]	This study
pKNSD125	pKNSD52 <i>PEX19</i> [1-75]	This study
pKNSD135	pKNSD52 <i>PEX19</i> [1-42]	This study
pKNSD98	pKNSD55 <i>PEX3</i>	This study
pKNSD132	pKNSD55 <i>PEX3</i> [1-110]	This study
pKNSD130	pKNSD55 <i>PEX3</i> [110-445]	This study
pKNSD121	pKNSD55 <i>PEX10</i>	This study
pKNSD173	pKNSD55 <i>PEX10</i> [1-380]	This study
pKNSD133	pKNSD55 <i>PEX10</i> [1-217]	This study
pKNSD134	pKNSD55 <i>PEX10</i> [193-217]	This study
pKNSD136	pKNSD55 <i>PEX10</i> [193-419]	This study
pKNSD171	pKNSD55 <i>PEX10</i> [260-419]	This study
pKNSD172	pKNSD55 <i>PEX10</i> [260-380]	This study
pKNSD174	pKNSD55 <i>PEX10</i> [217-380]	This study

Bacto-agar (2% wt/vol) was added for solid media. For oleate inductions, *P. pastoris* strains were grown in batch in mineral medium containing 0.2% (vol/vol) oleate and 0.02% (vol/vol) Tween 40 (MMOT) (Veenhuis *et al.*, 1979).

For the induction experiments (see Figures 3 and 8A) cells were precultured in MMG media (2% dextrose) and in the midlogarithmic phase shifted to MMM media (0.5% methanol) or MMOT media. PPY4 and SKF13 cultures were inoculated at an A₆₀₀ of 0.2 and 0.5, respectively. At the indicated times, cells were harvested, and total cellular extracts were prepared as described previously (Monosov *et al.*, 1996). Two to 20 μg of total protein were loaded per lane.

Molecular Biological Techniques

All plasmids used in this study are listed in Table 2. All DNA-oligonucleotide primers used are listed in Table 3.

Escherichia coli strains JM109, DH5α, and XL1blue were routinely used for propagation and amplification of plasmids and grown by standard methods. Enzyme digestions, cloning, plasmid isolation, PCRs, and Southern blotting were performed according to standard techniques (Sambrook *et al.*, 1989). All reagents were handled according to the manufacturer's instructions. DNA sequencing was performed by the method of Sanger *et al.* (1977).

P. pastoris transformations, mating, sporulation, and random spore analysis were performed as described (Gould *et al.*, 1992).

Isolation of Peroxisome Assembly (*pex*) Mutants

Isolation of *P. pastoris pex* mutant strains was based on the procedure originally described for *S. cerevisiae* (Elgersma *et al.*, 1993), and also for the *P. pastoris* screen for *pex* mutants defective in the import of PTS2-containing proteins (Elgersma *et al.*, 1998). The Tn5-BLE-

PTS1 gene from pEL43 (Elgersma *et al.*, 1993) was excised as a *Bam*HI fragment and inserted into the *Bam*HI site of pAM2F plasmid (a gift from J. Heyman, University of California, San Diego, CA) creating pTW2. Plasmid pAM2F is based on the plasmid pSG464 (Gould *et al.*, 1992) and contains a *S. cerevisiae* ARG4 gene, an autonomous-replicating sequence for *P. pastoris*, a 5' AOX promoter fragment, a 3' AOX transcription termination fragment, and a multiple-cloning site in between the 5' and 3' AOX fragments. This placed BLE-PTS1 under control of the methanol-inducible AOX1 promoter (Ellis *et al.*, 1985). This plasmid was transformed into PPY12, yielding strain STW3. A 100-ml culture of strain STW3 was grown in YPD to an A₆₀₀ of 1.0 and subjected to *N*-methyl-*N*-nitro-*N*-nitrosoguanidine mutagenic treatment as described (Elgersma *et al.*, 1998). The enrichment in 25 μg/ml phleomycin was as described previously (Elgersma *et al.*, 1998). Cells were then collected, washed, resuspended in 100 ml of YPD, and incubated for 2 h at 30°C. Subsequently, various dilutions were plated onto YPD agar. Cells were grown for 2 d and replica plated onto YNM plates. Methanol nonutilizers, putative *pex* mutants, were selected for further characterization.

Cloning and Sequencing of PEX19

A genomic library constructed in plasmid pYM8 (Liu *et al.*, 1995) was used to transform mutant strain *pex19-112*. Ten clones, p112-1 to p112-10, were identified, which complemented strain *pex19-112* for growth on methanol. Restriction analysis revealed four distinct, overlapping, genomic inserts. The complementing fragment was narrowed to a 2.2-kb *Sal*I fragment by subcloning into pSG560 (p112Sal). Approximately 1.4 kb of the *Sal*I fragment was sequenced (GenBank AF133271), which revealed a 900-bp ORF. The 1.4-kb fragment was amplified by PCR (Primers TW49 and TW59), cloned into pCRII (Invitrogen, Carlsbad, CA) (pTW119), excised with

Table 3. Primers

Name	DNA sequence (5' → 3')
KNF16	CCCGATTCTCAAATACAACCAAGAAGTACC
KNF21	CCCGGATCCATGCCCCATCTGAAGAGATC
KNF32	CCCGGATCCAAGAGGTTTTCTCCATGAGG
KNF33	CCCGAATTCCGTAGTTCCTCCATTGGTG
KNF39	CCCGGATCCTTACTAGGAGGGTTGATTG
KNF43	CGCGGCCGCCAAATTGGATAAGAACC
KNF44	CCCGAATCATCTAAGATTGGCAGATATG
KNF45	TCTCGAGTCTAGAGATATCTGAGGTAATGCAGGGAAC
KNF46	CCCGCGGCCGCAATCAAAAAGTACCCATCTC
KNF47	CGCGGCCGCCGATAACAATTTACACAC
KNF48	CCCGGAATTCATTTCCGAGACAGTTCGTTG
KNF49	AAGATCTGATATCTGACCAGTAATCATCTCTG
KNF50	CCCGCGGCCGCCAGACTGTAAACGTCAG
TW49	AAGTATCATGACTGCTG
TW59	GTGTGGAATTGTGAGCGG
TW61	GGATCCATGAGTAGCGAGGACGAAGTAC
TW63	GGATCCCTGCTGTTTACAAGTCTCATC
PEX10B	CCAGGATCCCAGAAATCAATCAAAAAGTACC
PEX10C	GCCGGATCCATGCCCCATCTGAAG
PEX19up	GCGGAGCTCAATTTACACAGGTAACACAGC
PEX19dn	GCGTGTACTGCTGTTTACAAGTCTC
SAAX.19	GCGTGTACTGCTGTTTACTAGTCTCATCC
ΔC4.19	GCGTGTACTGCTCATCCAATTCCTTGC

*Bam*HI and *Xho*I, and cloned directly into pSG560 (Gould *et al.*, 1992), yielding pTW121. This plasmid complemented *pex19* deletion strains for growth on methanol and oleate media, confirming that this region comprised the *PEX19* ORF and the required regulatory elements.

Two-Hybrid Analysis

Cloning vectors, tester strains, and screening by two-hybrid analysis, as well as two-hybrid vectors containing full-length *PEX3*, have been described (Faber *et al.*, 1998). A full-length clone of *PEX10* was amplified by PCR (primers KNF16 and KNF21) and inserted as a *Bam*HI-*Eco*RI DNA fragment in pKNSD55, creating pKNSD121. A full-length clone of *PEX19* was generated by cloning the *Bam*HI fragment from pTW119 (see above) into pKNSD52 cut with the same enzyme, creating pKNSD123. Fragments of *PEX3* and *PEX19* were introduced in pKNSD55 and pKNSD52, making use of matching restriction sites present in the ORF of these genes and the vectors: *PEX3*[1–110] generated with *Bam*HI creates pKNSD132; *PEX3*[110–445] generated with *Bam*HI creates pKNSD130; *PEX19*[1–42] generated with *Bgl*II creates pKNSD135; *PEX19*[1–75] generated with *Pst*I creates pKNSD125; and *PEX19*[1–232] generated with *Eco*RI creates pKNSD127. Fragments of *PEX10* were cloned into pKNSD55 as follows. *PEX10*[1–217] was amplified by PCR (primers KNF21 and KNF33), cut with *Bam*HI and *Eco*RI, and inserted into pKNSD55 cut with the same, creating pKNSD133. *PEX10*[193–217] was amplified by PCR (primers KNF32 and KNF33), cut with *Bam*HI and *Eco*RI, and inserted into pKNSD55 cut with the same, creating pKNSD134. *PEX10*[193–419] was amplified by PCR (primers KNF16 and KNF32), cut with *Bam*HI and *Eco*RI, and inserted into pKNSD55 cut with the same, creating pKNSD136. *PEX10*[1–380] was generated by cutting pKNSD121 with *Sal*I and religating to create pKNSD173. *PEX10*[217–419] was amplified by PCR (primers KNF16 and KNF39), cut with *Bam*HI and *Eco*RI, and inserted into pKNSD55 cut with the same, creating pKNSD170. *PEX10*[260–419] was generated by cutting pKNSD170 with *Eco*RV and *Eco*RI and the 490-bp fragment cloned into pKNSD53 cut with *Bam*HI (blunted by Klenow) and *Eco*RI, creating pKNSD171.

PEX10[260–380] was generated by cutting pKNSD170 with *Sal*I and *Eco*RI and the 490-bp fragment cloned into pKNSD53 cut with *Bam*HI, blunted by Klenow polymerase, and *Sal*I, creating pKNSD172. *PEX10*[217–380] was generated by cutting pKNSD170 with *Sal*I and religating to create pKNSD174.

Construction of *pex19Δ* Strains

The 5' and 3' flanking regions, 300 and 250 bp, respectively, of the *PEX19* ORF were amplified by PCR (primers KNF47, KNF48, KNF49, and KNF50) and inserted into pBluescript II KS+ (Stratagene, La Jolla, CA), cut with *Xba*I (blunted by Klenow polymerase) and *Not*I for the 3' region and with *Asp*7181 (blunted by Klenow polymerase) and *Eco*RI for the 5' region. This created a *Not*I site at both the extreme 5' and 3' ends, resulting in plasmid pKNSD168. The *ZEO* gene was cut from plasmid pPICZa (Invitrogen) as a 0.9-kb *Bam*HI-*Stu*I DNA fragment and cloned between the 5' and 3' *PEX19* fragments in plasmid pKNSD168, digested by *Bam*HI and *Eco*RV, resulting in pKNSD169. The disruption cassette was subsequently excised from pKNSD169 cut with *Not*I and used to transform PPY12, SMD1163, and STW2. Transformants were selected on YPD plates containing 100 μg/ml Zeocin (Invitrogen, Carlsbad, CA), and the expected genomic alteration in *pex19* deletion strains, which were unable to grow on methanol, was confirmed by Southern blot analysis (our unpublished data).

Construction of the Farnesylation Mutants

Plasmid pWSP50 was generated by cloning the PCR (primers PEX19up and PEX19dn) product into pCR-Blunt (Invitrogen), excising with *Bam*HI and *Eco*RI, and ligating to pIB1 (Sears *et al.*, 1998), a *HIS4* integrating vector, cut with the same enzymes. pWSP51 and pWSP52 were cloned using the same method as for pWSP50 using unique downstream primers (SAAX.19 and ΔC4.19). The *pex19C296S* mutation was confirmed by cutting at the unique restriction site (*Spe*I) that was introduced along with the codon change. These plasmids were introduced into SKF14 after linearization with *Sal*I.

Preparation of Rabbit Anti-PpPex19p Antibodies

The *PEX19* ORF was amplified by PCR (primers TW61 and TW63), introducing *Bam*HI sites immediately 5' and 3' of the ORF, and cloned as a *Bam*HI fragment into pQE9 (Qiagen, Chatsworth, CA) yielding plasmid pTW128. Amino-terminally *HIS*₆-tagged PpPex19p was purified from *E. coli* using the manufacturer's procedures for denatured proteins. Quantitative amounts of *HIS*₆-PpPex19p were eluted from SDS-polyacrylamide gels and used to immunize rabbits (Bob Sergeant, Ramona, CA).

Biochemical Techniques

Crude cell-free extracts for Figure 9 were made as described previously (Babst *et al.*, 1997). SDS-PAGE (Laemmli, 1970) and Western blot analyses (Towbin *et al.*, 1979) were performed as described. Goat anti-rabbit HRP or goat anti-rabbit alkaline phosphatase (Bio-Rad, Hercules, CA) were used as secondary antibodies, which were detected by ECL (Amersham, Arlington Heights, IL) or bromochloroindoyl phosphate/nitro blue tetrazolium (Kirkland & Perry, Gaithersburg, MD) according to the manufacturers' protocols. Primary antibodies and the dilutions used were α-Pex19p (1:4000), α-Pex3p (1:10,000), α-ScTHIO (1:10,000), α-CAT (1:10,000), α-MOX (1:10,000), α-Pex5p (1:10,000), α-Sc-glucose-6-phosphate dehydrogenase (1:2000), and mouse-α-NH (1:5).

Immunoprecipitation was performed from 5 A₆₀₀ units of cells in Tris-buffered saline and 0.5% Triton X-100 with 2 μl of anti-Pex19p per reaction as described previously (Stack *et al.*, 1993).

Subcellular Fractionation Experiments

Differential centrifugation of oleate-grown cells was performed as described (Faber *et al.*, 1998), except that 100 A₆₀₀ units of cells were lysed in 5 ml of lysis buffer. Fractionations of methanol-grown cells were performed as with the oleate-grown cells, except that a HEPES-KOAc buffer (0.2 M sorbitol, 50 mM KOAc, 2 mM EDTA, and 20 mM HEPES, pH 6.8) was used as the lysis buffer. For floatation, all sucrose stocks contained the HEPES-KOAc buffer lacking the sorbitol, and the gradients were prepared as follows: 0.5 ml of postnuclear supernatant (PNS) from the methanol-grown cells was mixed with 1.5 ml of 80% (wt/vol) sucrose in a 5-ml ultracentrifuge tube; this was layered with 1.5 ml of 55% (wt/vol) sucrose and then 1.5 ml of 35% (wt/vol) sucrose. The gradients were centrifuged in a Beckman (Palo Alto, CA) SW50.1 rotor for 20 h at 40,000 rpm; 950- μ l fractions were collected from the top and adjusted to 5% trichloroacetic acid (TCA). The material pelleted on the bottom of the tube was resuspended in 1 ml of 5% TCA and transferred to an Eppendorf tube. The TCA precipitations were incubated on ice for >20 min and washed once with 5% TCA and three times with cold acetone. The acetone was evaporated, and the pellets were resuspended in 100 μ l of SDS-PAGE sample buffer.

Construction of a Strain Expressing NH-Pex10p

A *pex10 Δ* construct was made as follows. The 3' region of *PEX10* was amplified by PCR (primers KNF45 and KNF46), cut with *NotI*, and ligated to pBluescript II KS+ cut with *XbaI* (filled in with Klenow) and *NotI*, creating pKNSD164. The 5' region of *PEX10* was amplified by PCR (primers KNF43 and KNF44), cut with *NotI*, and ligated to pKNSD164 cut with *Asp718I* (filled in with Klenow) and *EcoRI*, creating pKNSD167. The *ZEO* gene was released from pPICZa (Invitrogen) with *StuI* and *BamHI* and ligated into pKNSD167 cut with *SmaI* and *BamHI*, creating pSH5. pSH5 was cut with *NotI* and transformed into strain SMD1163 to create the *pex10 Δ* strain SSH4, which was confirmed by genomic PCR and unable to grow on methanol- or oleate-containing medium. *PEX10* was amplified by PCR (primers PEX10B and PEX10C), cut with *BamHI* and *EcoRI*, and inserted into p21-43 cut with the same, creating pSSH38. p21-43 was a gift of Ype Elgersma (University of California, San Diego, CA) and has the acyl-coenzyme A oxidase promoter upstream of a *BglIII*-*BamHI* fragment encoding the NH epitope (Elgersma *et al.*, 1996), with a downstream *EcoRI* site, and the *HIS4* gene for selection in *P. pastoris*. pSSH18 was cut with *StuI* and integrated into SMD1163 creating strain SSH18.

Fluorescence and Electron Microscopy

Preparation and analysis of cells expressing green fluorescent protein (GFP) constructs were as described (Monosov *et al.*, 1996). Samples for immunofluorescence were prepared from methanol-induced cells spheroplasted as described for biochemical fractionation and then fixed and prepared as described previously (Babst *et al.*, 1998). Pex3p and catalase antibodies were used at dilutions of 1:10,000. Microscopy for Figure 5 is as described (Odorizzi *et al.*, 1998). Immunofluorescence was visualized on a Delta Vision (Issaquah, WA) optical sectioning microscope (Pogliano *et al.*, 1999) for Figure 6. Cells for electron microscopy were prepared as described previously (Sakai *et al.*, 1998).

RESULTS

A Positive Selection Yields New *pex* Mutants

To characterize novel *PEX* genes encoding proteins required for peroxisomal protein import, we applied a positive-screening method, originally described for *S. cerevisiae* (Elgersma *et al.*, 1993), in *P. pastoris*. This procedure uses a drug resistance protein fused to a

PTS to select mutants; in wild-type cells the drug resistance protein hybrid is imported into the peroxisome, and the cells are sensitive to the drug. Import mutants accumulate the resistance protein hybrid in the cytosol and thus become resistant to the drug. To this end, the gene encoding the bleomycin-resistance protein BLE from the Tn5 transposon was fused with a carboxyl-terminal PTS1 encoding sequence (-SKL) and placed under control of the *P. pastoris* alcohol oxidase 1 promoter. After *N*-methyl-*N*-nitro-*N*-nitrosoguanidine mutagenesis of the strain carrying this construct and enrichment of mutants (see MATERIALS AND METHODS) that were defective for the import of the reporter protein into the peroxisome, several hundred candidate colonies were obtained. Twenty-two of these strains were unable to grow on oleate or methanol as the sole carbon source but grew well on media containing glucose, glycerol, or ethanol, indicating the specificity of the peroxisome defect. These strains were crossed with available *pex* mutants and assigned to complementation groups. Most mutants fell into known complementation groups (Table 4). However, one mutant (112) did not belong to any of the existing *P. pastoris pex* complementation groups and accumulated both PTS1- and PTS2-containing GFP fusion proteins in the cytosol (our unpublished data). Accordingly, this mutant was chosen for further analysis.

Cloning of *P. pastoris PEX19*

Complementation of the methanol growth defect of mutant 112 by a genomic DNA library led to the identification of four distinct clones that contained overlapping genomic inserts (our unpublished data). The minimal complementing region was narrowed to a 2.2-kb *SalI* fragment (our unpublished data). Sequence analysis revealed an ORF of 897 nucleotides (GenBank accession number AF133271), encoding a 299-amino acid protein (Figure 1) with a predicted molecular mass of 33.7 kDa. This protein is predicted

Table 4. Complementation groups of new *P. pastoris pex* mutants

Complementation group	No. of mutants found
<i>PEX1</i>	1
<i>PEX2</i>	2
<i>PEX3</i>	2
<i>PEX4</i>	0
<i>PEX5</i>	4
<i>PEX6</i>	2
<i>PEX8</i>	4
<i>PEX10</i>	0
<i>PEX12</i>	6
<i>PEX13</i>	0
Unknown	1



Figure 1. Sequence alignment of Pex19p orthologues. The amino acid sequences were aligned using the ClustalW program. Identical residues (black) and similar residues (gray) in at least half of the orthologues are shaded. Pp, *P. pastoris* Pex19p; Sc, *S. cerevisiae* Pex19p; Hs, *Homo sapiens* HK33/PxP; Cg, *Cricetulus griseus* PxP; Sp, *S. pombe* hypothetical protein C17C9.14; Ce, *C. elegans* hypothetical protein F54F2.8. Similarity rules: G = A = S, A = V, V = I = L = M, I = L = M = F = Y = W, K = R = H, D = E = Q = N, and S = T = Q = N. Dashes represent gaps.

to be negatively charged (pI 3.88) and hydrophilic, lacking recognizable hydrophobic transmembrane domains. Comparison of the protein sequence with those in databases revealed five proteins with significant homology, namely Chinese hamster PxF (James *et al.*, 1994), human PxF (Kammerer *et al.*, 1997) (originally called HK33; Braun *et al.*, 1994), *S. cerevisiae* Pex19p (Götte *et al.*, 1998), and uncharacterized ORFs from *Schizosaccharomyces pombe* and *Caenorhabditis elegans* (Figure 1). The similarity among these proteins suggests that the complementing fragment encodes the *P. pastoris* PEX19. All previously described PxF/Pex19p proteins have been shown to be farnesylated at a carboxy-terminal sequence, CaaX (C, cysteine; a, aliphatic; X, any amino acid). Notably, Pex19p contains a CKQQ residue at the carboxyl terminus that is fully conserved between *S. cerevisiae* and *P. pastoris*.

Peroxisome Protein Synthesis and Localization Defects in the pex19Δ Mutant

P. pastoris strains deleted for PEX19 were constructed as described in MATERIALS AND METHODS. These

pex19Δ mutants were unable to grow on methanol or oleate as sole carbon sources (see below) and mislocalized catalase, a PTS1-containing peroxisome matrix protein, and PTS2-GFP proteins in the cytosol (Figure 2), indicating a defect in the import of both PTS1- and PTS2-containing peroxisome matrix proteins. In contrast, wild-type cells showed the characteristic punctate peroxisomal staining pattern (Figure 2).

To characterize protein synthesis and stability defects in the *pex19Δ* mutant, wild-type and *pex19Δ* cells were grown in peroxisome-inducing conditions, and the steady-state levels of peroxisomal proteins was determined by SDS-PAGE and immunoblotting. In oleate-grown wild-type cells, a characteristic induction pattern is observed for Pex3p, Pex5p, and thiolase (Figure 3A). In contrast, the *pex19Δ* cells contained lower levels of Pex3p, a PMP, after 4 h of induction when compared with wild-type cells (Figure 3A). The initial levels of Pex3p appeared normal during the first 2 h of induction, suggesting that the defect at later time points is not due to lower induction of Pex3p synthesis in oleate media. Pex5p and thiolase were

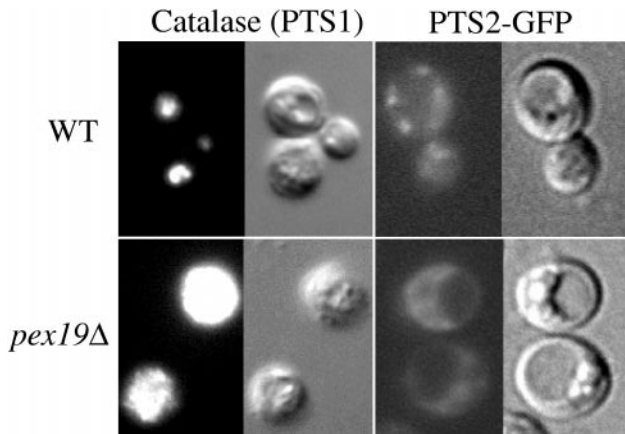


Figure 2. *pex19Δ* mutants are defective for the import of catalase (PTS1) and PTS2-GFP. Wild-type and *pex19Δ* cells (SMD1163 and SKF14) grown in methanol media were prepared for anti-catalase immunofluorescence, and PTS2-GFP expressing wild-type and *pex19Δ* cells (STW2 and AK11) grown in oleate media were visualized using a fluorescence microscope (anti-catalase, GFP) and Nomarski optics as described in MATERIALS AND METHODS.

present at near wild-type levels in *pex19Δ* mutants throughout the oleate induction, suggesting that induction of peroxisomal proteins is normal in *pex19Δ* mutants. The internal loading control, mitochondrial $F_1\beta$ -ATPase, was similar in all samples. In methanol-grown cells no significant difference was observed between wild-type and *pex19Δ* cells for the levels of Pex3p, alcohol oxidase (MOX), and Pex5p (Figure 3B). These results suggest that there is a defect in the biogenesis of Pex3p, which could lead to protein instability, in oleate-grown *pex19Δ* cells.

Differential centrifugation of a lysate prepared from oleate-induced wild-type and *pex19Δ* cells (see MATERIALS AND METHODS) confirmed the peroxisome protein import defect of *pex19Δ* cells (Figure 4). PTS1-

and PTS2-containing proteins catalase and thiolase were detected in the lysate or PNS after a low-speed spin (Figure 4A). Upon centrifugation at $27,000 \times g$, the pellet fraction from wild-type cells contained peroxisome-associated catalase, thiolase, and the membrane protein Pex3p (P27). Some of the catalase and thiolase leaked from the peroxisome during the biochemical manipulations, consistent with previous reports (Kalish *et al.*, 1996; Waterham *et al.*, 1996; Elgersma *et al.*, 1998; Faber *et al.*, 1998), and could not be further pelleted even at $100,000 \times g$. In contrast, in *pex19Δ* cells thiolase and catalase were found exclusively in the supernatant fractions (Figure 4A, S27 and S100). The PMP Pex3p could not be detected in oleate-grown cells (Figure 4A; also see Figure 3A). These data clearly demonstrate a defect for the import of luminal peroxisomal proteins containing PTS1 or PTS2 sequences in *pex19Δ* mutants.

To follow the fate of Pex3p in the absence of Pex19p, a fractionation experiment was performed with methanol-grown cells. We observed the majority of Pex3p in the $27,000 \times g$ and $100,000 \times g$ pellet fractions (P27 and P100) of both wild-type and *pex19Δ* cells (Figure 4B). The S100 and P100 pools of Pex3p are likely due to the increased rupture of methanol-grown peroxisomes, compared with oleate-grown peroxisomes, during the fractionation procedure, a phenomena that has been observed previously with luminal peroxisomal proteins (Waterham *et al.*, 1996). To determine whether the Pex3p that pellets in the *pex19Δ* cells is membrane associated, or simply in large protein aggregates, we loaded a PNS fraction at the bottom of a sucrose density gradient to see whether Pex3p could float to lighter-density fractions, a behavior that is consistent with membrane association. A large portion of Pex3p from both strains floated from the load fractions (Figure 4C, lanes 1 and 2), which contain 60% sucrose, to the float fractions (Figure 4C, lanes 3 and

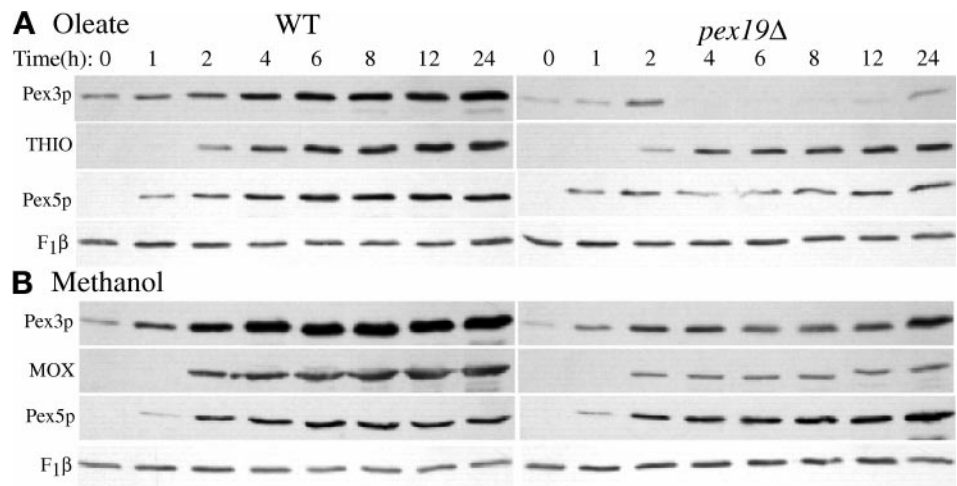


Figure 3. Steady-state levels of peroxisomal proteins during oleate and methanol growth of wild-type and *pex19Δ* cells. Glucose-grown wild-type and *pex19Δ* cells (PPY12 and SKF13) were shifted to oleate (A) or methanol media (B), and samples were collected at the indicated times and processed as described in MATERIALS AND METHODS for SDS-PAGE and immunoblotting with the indicated antibodies.

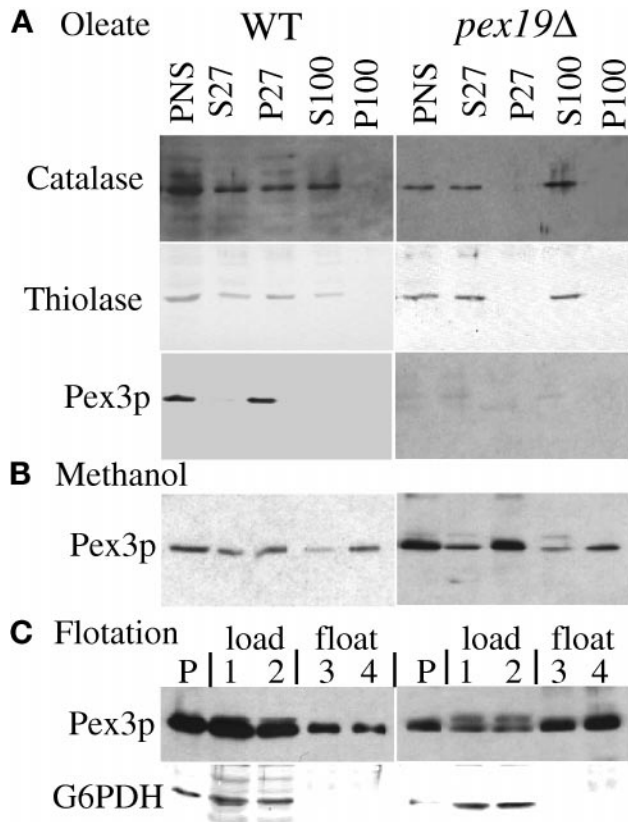


Figure 4. Mislocalization of peroxisomal proteins by *pex19Δ* mutants. Oleate-grown (A) and methanol-grown (B) spheroplasts of wild-type and *pex19Δ* cells (SKF14 and SMD1163) were lysed and subjected to sequential differential centrifugation. Equivalent amount of the PNS, 27,000 × g supernatant (S27), 27,000 × g pellet (P27), 100,000 × g supernatant (S100), and 100,000 × g pellet (P100) were resolved by SDS-PAGE, transferred to nitrocellulose, and probed with the indicated antibodies. (C) The PNS from methanol-grown cells was adjusted to 60% sucrose, layered with 55 and 35% sucrose, and centrifuged to allow floatation of membranes into the lighter fractions as described in MATERIALS AND METHODS. P, pelleted material at the bottom of the tube. Fractions are numbered from the bottom to the top and were collected as described in MATERIALS AND METHODS. Fractions 1 and 2 are the 60% sucrose load zone; fractions 3 and 4 are the 55% sucrose float zone. The top fraction contained no protein.

4), which contain 55% sucrose. Very little detectable Pex3p was found in the very top fraction of the gradient containing 35% sucrose, and some of the Pex3p was pelleted to the bottom of the tube (Figure 4C, lanes P). The cytosolic protein glucose-6-phosphate dehydrogenase did not float into fractions that contain 55% sucrose (Figure 4C) as expected. This analysis suggests that at least a portion of Pex3p is localized to membranous structures in *pex19Δ* cells grown in methanol medium.

Novel Peroxisome Remnants in *pex19Δ* Cells

Methanol-induced wild-type and *pex* mutant cells were analyzed for the presence of peroxisomal rem-

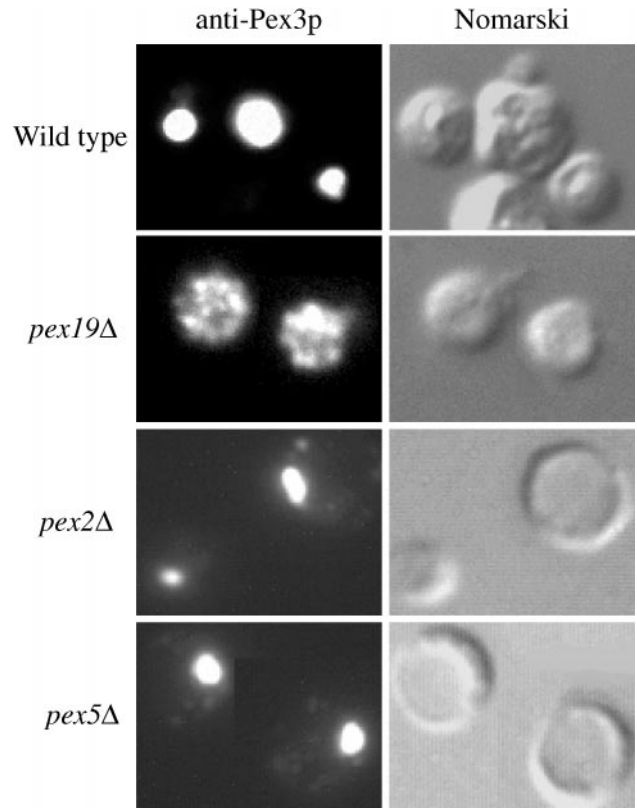


Figure 5. Immunofluorescence microscopy of Pex3p-containing compartments in wild-type and *pex* mutant cells. Methanol-grown wild-type (PPY12), *pex19Δ* (SKF13), *pex2Δ* (PPY12Δ2), and *pex5Δ* (PPY12Δ5) spheroplasts were indirectly labeled with the anti-Pex3p antibody and visualized by fluorescence microscopy (Pex3p) and Nomarski optics.

nants by using indirect immunofluorescence to visualize Pex3p-containing structures. In wild-type cells the characteristic large cluster of peroxisomes was observed, which contain Pex3p (Figure 5). In *pex2Δ* and *pex5Δ* mutants, a large cluster of peroxisome remnants, or ghosts, was observed (Figure 5). Similar structures were observed in all other *pex* mutants examined, including *pex1*, 4, 6, 7, 8, 10, 12, and 13 (Gould *et al.*, 1992, 1996; McCollum *et al.*, 1993; Spong and Subramani, 1993; Heyman *et al.*, 1994; Kalish *et al.*, 1995, 1996; Liu *et al.*, 1995; Waterham *et al.*, 1996; Elgersma *et al.*, 1998; Snyder, unpublished results). In contrast, *pex19Δ* cells did not contain the large cluster of organelle remnants, but instead Pex3p was found in small bright dots dispersed throughout the cell (Figure 5). To further elucidate the morphology of the Pex3p-containing structures in *pex19Δ* cells, Pex3p immunofluorescence was visualized in a deconvolution microscope, which provides greater resolution, allowing the visualization of peroxisome membrane staining by Pex3p antibodies in wild-type cells (Figure 6A). In contrast, the Pex3p-containing structures in *pex19Δ*

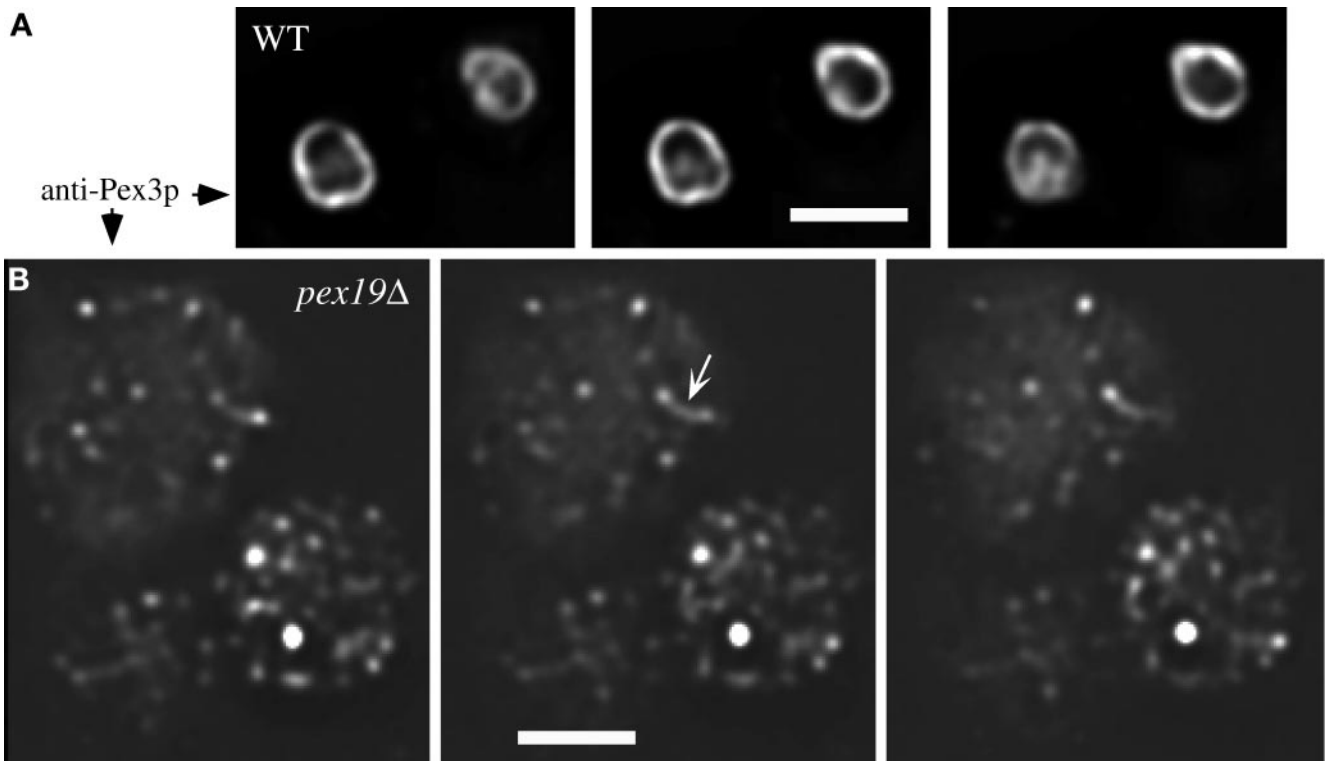


Figure 6. Deconvolution microscopy of Pex3p immunofluorescence from wild-type and *pex19Δ* cells. Pex3p-containing compartments from wild-type (PPY12) (A) and *pex19Δ* (SKF13) (B) cells were visualized by immunofluorescence staining with Pex3p antibodies on a Delta Vision optical sectioning microscope. Three consecutive 0.2- μ m sections are shown from each strain. Bar, 2 μ m.

cells appeared as very small spheres and tubules (Figure 6B). The arrowhead in Figure 6B points to one such tubule that seems to be connecting two of the small spherical structures. These results and those presented above support the conclusion that Pex3p is localized to small spherical and tubular membranous compartments in the absence of Pex19p, and that these structures are smaller and more dispersed than the typical peroxisome ghosts seen in other *P. pastoris* *pex* mutants.

Analysis of the methanol-induced *pex19Δ* cells by electron microscopy revealed structures that were absent in wild-type cells (Figure 7, compare A and B). These structures are small vesicles and tubules (Figure 7C), which likely correspond to the Pex3p-containing structures seen in the immunofluorescence experiment. Immunoelectron microscopy revealed clusters of gold particles when stained with Pex3p antisera; however, no membranous structures were visualized around these clusters because of insufficient contrast or resolution (our unpublished data). The data presented above clearly indicate the presence of Pex3p-containing peroxisome remnants in *pex19Δ* cells, but our inability to clearly visualize such structures by electron microscopy demonstrates the difficulties with

identification of certain types of peroxisome remnants by this technique.

Characterization of Pex19p and Its Predominantly Cytosolic Location

Rabbit antibodies were raised against bacterially expressed HIS₆-tagged Pex19p. These antibodies specifically recognized a single protein band of ~45 kDa in wild-type cells, which was absent in the *pex19Δ* strain (see below). Like many Pex proteins, Pex19p was detectable in glucose-grown cells and was induced 5- to 10-fold during peroxisome-inducing conditions (Figure 8A). The observed molecular weight of Pex19p was significantly different from the calculated molecular mass of 33.7 kDa but is in agreement with the molecular mass observed for the bacterially expressed protein (our unpublished data) and is the same for oleate- and methanol-grown cells. Therefore, the reduced migration in SDS-PAGE seems to be an intrinsic feature of Pex19p. Notably, only a single species of Pex19p was observed in either growth condition.

The subcellular localization of Pex19p was determined by the differential fractionation technique. Controls for this experiment are shown in Figure 4A,

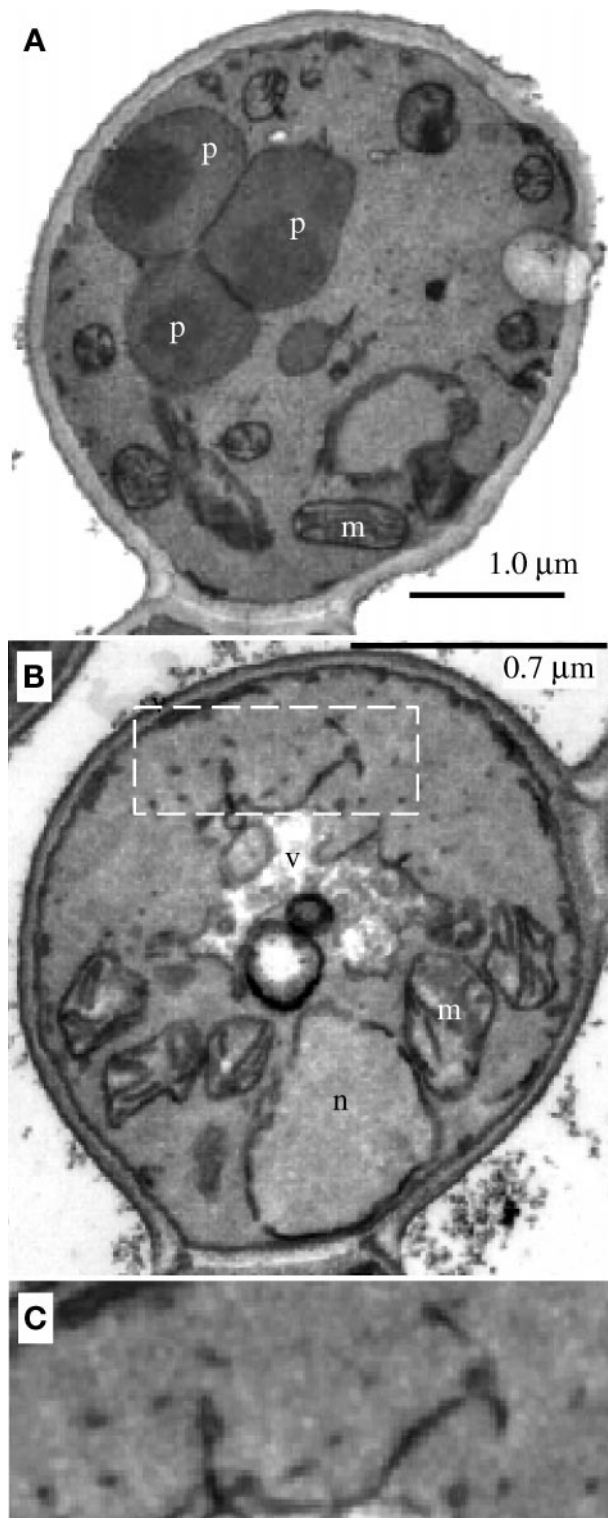


Figure 7. Electron microscopy of wild-type and *pex19* Δ cells. Methanol-grown wild-type (PPY12) (A) and *pex19* Δ (SKF13) (B) cells were prepared as described in MATERIALS AND METHODS. (C) Enlargement of the area highlighted by dashed white box in B. n, nucleus; m, mitochondria; v, vacuole; p, peroxisome.

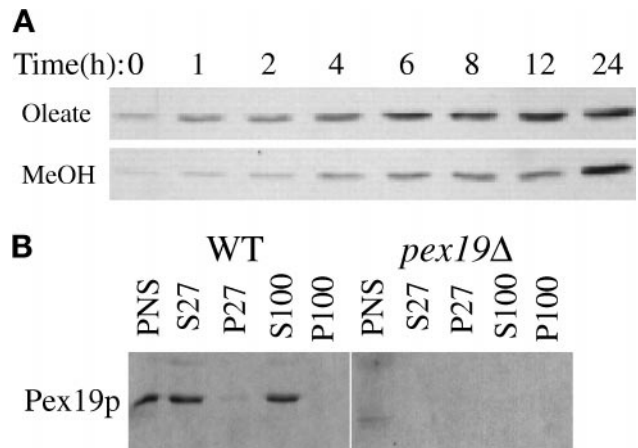


Figure 8. Induction and subcellular fractionation of Pex19p. (A) Glucose-grown wild-type cells (PPY12) were shifted to oleate and methanol media, and samples were collected at the indicated times and processed as described for Figure 3 for immunoblotting with anti-Pex19p antibodies. (B) Oleate-grown spheroplasts of wild-type and *pex19* Δ cells (SMD1163 and SKF14) were lysed and subjected to sequential differential centrifugation. Equivalent amounts of the PNS, 27,000 \times g supernatant (S27), 27,000 \times g pellet (P27), 100,000 \times g supernatant (S100), and 100,000 \times g pellet (P100) were resolved by SDS-PAGE, transferred to nitrocellulose, and probed with anti-Pex19p antibodies.

where peroxisome marker proteins fractionated in the usual manner. Centrifugation of the PNS at 27,000 \times g left Pex19p predominantly (>95%) in the supernatant fraction (Figure 8B, S27). Minor amounts (<5%) of Pex19p were present in this organelle pellet fraction (Figure 8B, P27), consistent with this pool of Pex19p being localized to the peroxisome. Further centrifugation of the 27,000 \times g supernatant at 100,000 \times g did not pellet any of the Pex19p, suggesting that the protein is predominantly cytosolic (Figure 8B, S100 and P100). The absence of the Pex19p band in *pex19* Δ cells indicates the specificity of the antibody (Figure 8B).

The Putative Farnesylation Site Is Not Essential for Protein Function

All members of the PxF/Pex19p family examined so far are known to be farnesylated at a carboxyl-terminal CaaX motif (James *et al.*, 1994; Kammerer *et al.*, 1997; Götte *et al.*, 1998). Moreover, in *S. cerevisiae* the farnesylation site was important for protein function but not absolutely required; a mutant form of Pex19p, with a serine replacing the cysteine four amino acids from the carboxyl terminus (ScPex19pC347S), can partially complement the deletion mutant for growth on oleate media and shows partial localization of peroxisomal markers (Götte *et al.*, 1998). This SaaX-containing mutant protein is not a substrate for farnesylation. PpPex19p also contains the same carboxyl-terminal four amino acids as ScPex19p. To test whether this

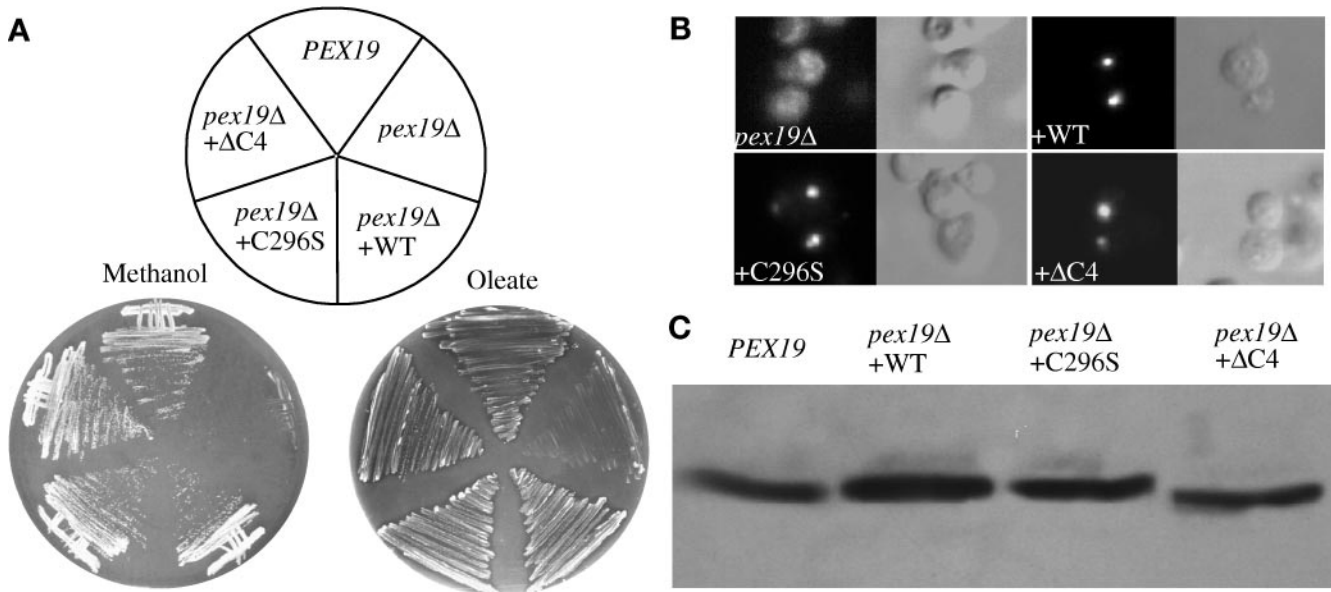


Figure 9. The putative farnesylation site is not essential for Pex19p function. (A) Cells were grown on plates supplemented with methanol (left panel) or oleate (right panel) as sole carbon source. (B) Indirect immunofluorescence for catalase in methanol-grown *pex19Δ* cells and *pex19Δ* cells transformed with the indicated Pex19p-expressing plasmids. (C) Western blot analysis of total extracts of methanol-grown cells probed with Pex3p antibodies. *PEX19*, wild-type (SMD1163); *pex19Δ*, deletion mutant (SKF14); *pex19Δ* + WT, deletion mutant transformed with the wild-type *PEX19* (WSP50); *pex19Δ* + C296S, deletion mutant transformed with the *pex19C296S* allele (WSP51); *pex19Δ* + Δ C4, deletion mutant transformed with the *pex19C296ter* allele (WSP52).

sequence is essential for protein function in *P. pastoris*, we deleted the four carboxyl-terminal amino acids (*pex19C296ter*) and also mutated the critical cysteine residue to serine (*pex19C296S*) and expressed these proteins from their own promoter, integrated in the chromosome of *pex19Δ* cells. Both mutant proteins complemented the *pex19Δ* phenotype for growth on methanol and oleate media (Figure 9A) and for the import of catalase into peroxisomes (Figure 9B). The mutant proteins were expressed at wild-type levels (Figure 9C). In addition, the Pex19pC296S displayed the same electrophoretic mobility as the wild-type protein (Figure 9C), and because the farnesylated form of the ScPex19p migrates faster in SDS-PAGE than the unmodified form (Götte *et al.*, 1998), we conclude that PpPex19p is not farnesylated under the conditions tested.

Pex19p Interacts with *Pex3p* and *Pex10p*

The yeast two-hybrid system was used to assay for potential protein-protein interactions between Pex19p and other peroxins from a collection of *PEX* gene two-hybrid constructs. A combination of a Pex19p-activation domain fusion protein with Pex3p- or Pex10p-DNA-binding domain fusions, both PMPs, resulted in activation of transcription of the reporter genes (*HIS3* and *LacZ*/ β -galactosidase) (Figures 10 and 11). Unfortunately, the two-hybrid analysis could only be tested with *PEX19* in the activation domain

plasmid, because this protein alone confers activation of transcription of the reporter genes when expressed as a DNA-binding domain fusion protein in the absence of an activation domain fusion (our unpublished data).

Mapping of the Protein-Protein Interaction Domains

The interacting domains of Pex3p and Pex19p were mapped by expressing subdomains of both proteins in

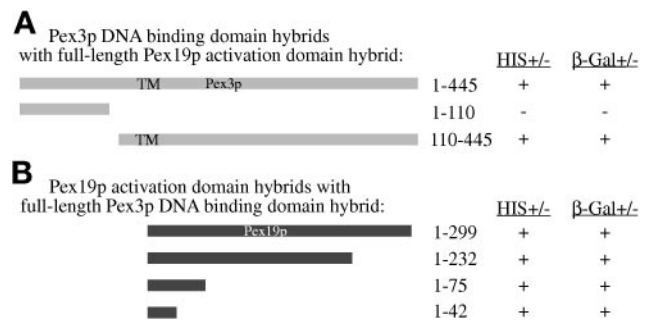


Figure 10. Two-hybrid analysis of Pex3p and Pex19p. The indicated Pex3p and Pex19p hybrid protein constructs were tested for trans-activation of the *HIS3* gene, resulting in growth on media lacking histidine (+) or *LacZ*, resulting in the production of β -galactosidase assayed by blue color change (+) as described in MATERIALS AND METHODS. Numbers refer to amino acids from Pex3p (A) or Pex19p (B). TM, relative position of the putative transmembrane domain in Pex3p.

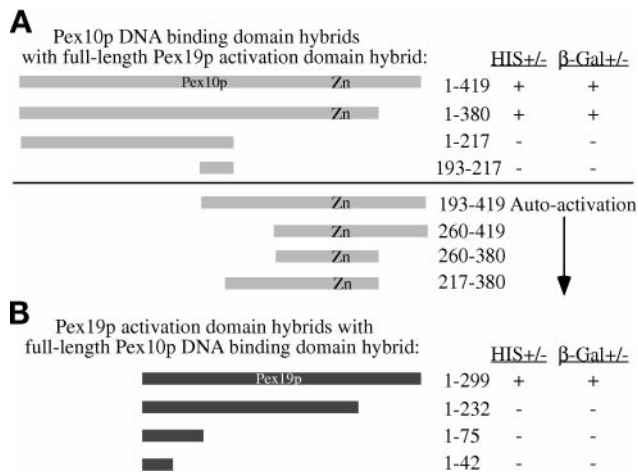


Figure 11. Two-hybrid analysis of Pex10p and Pex19p. The indicated Pex10p and Pex19p hybrid protein constructs were tested for trans-activation of the *HIS3* gene, resulting in growth on media lacking histidine (+) or *LacZ*, resulting in the production of β -galactosidase assayed by blue color change (+) as described in MATERIALS AND METHODS. Numbers refer to amino acids from Pex10p (A) or Pex19p (B). Zn, relative position of the zinc-binding domain in Pex10p.

the yeast two-hybrid system. Two subdomains of Pex3p, expressed as DNA-binding domain fusions, were tested for interaction with the full-length Pex19p-activation domain protein. The amino-terminal domain of Pex3p (amino acids 1–110) did not activate transcription of the reporter genes when expressed with the full-length Pex19p-activation domain fusion protein (Figure 10A). The carboxyl-terminal region, from amino acids 110–440, did result in activation of both reporter genes (Figure 10A) in the presence of the Pex19p-activation domain fusion protein. None of the Pex3p containing DNA-binding domain fusions autoactivated transcription from the reporter genes. The region of Pex19p responsible for the interaction with Pex3p was narrowed to the extreme amino terminus of Pex19p. Only 42 amino acids of the amino terminus of Pex19p were required to yield a positive interaction with the full-length Pex3p (Figure 10B). These results indicate that the amino terminus of Pex19p interacts with the carboxyl-terminal 335 amino acids of Pex3p in the two-hybrid system.

Pex10p domains were expressed in the two-hybrid system to further elucidate the site of interaction with Pex19p. DNA-binding domain fusions comprising many different regions of Pex10p were created with the goal of precisely mapping the interacting region; however, many of these fusion proteins led to the activation of transcription in the absence of an activation domain fusion (Figure 11A). The ability of these DNA-binding domain fusions to autoactivate transcription made the two-hybrid test impossible, because the DNA-binding domain fusions to Pex19p

also autoactivate transcription. A few of the Pex10p fusions do not autoactivate and were therefore useful to narrow the region of interaction to a domain between amino acids 1 and 380 (Figure 11A). The shorter amino-terminal fusion (amino acids 1–217) and the internal fragment (amino acids 193–217) that did not activate were not useful for a positive evidence-based conclusion. Moreover, only the full-length Pex19p fusion interacted with the full-length Pex10p fusion in the two-hybrid test (Figure 11B). Taken together these results suggest that a region of Pex10p, excluding the carboxyl-terminal 40 amino acids, interacts with Pex19p in a manner that is dependent on the extreme carboxyl terminus of Pex19p.

The interactions suggested by the two-hybrid system were confirmed by coimmunoprecipitation. We created a strain expressing an epitope-tagged version of Pex10p, NH-Pex10p, that fully complements a *pex10 Δ* mutant (our unpublished data). Oleate-induced wild-type, *pex19 Δ* , and *NH-PEX10* cells were lysed, and Pex19p was immunoprecipitated from these lysates. The material from the immunoprecipitation was separated by SDS-PAGE and immunoblotted to identify other Pex proteins in a complex with Pex19p. Pex19p was easily detected in these immunoprecipitations from wild-type and *NH-PEX10* strains but not from the *pex19 Δ* cells (Figure 12A). Pex3p was also observed in the Pex19p immunoprecipitations from wild-type and *NH-PEX10* strains but not from the *pex19 Δ* cells (Figure 12B) as expected. We also observed coimmunoprecipitation of NH-Pex10p with Pex19p antisera (Figure 12C) in the *NH-PEX10* strain. Pex19p immunoprecipitations did not contain detectable levels of Pex8p or Pex5p (our unpublished data), indicating the specificity of the result. These results demonstrate that Pex19p physically interacts with Pex3p and Pex10p.

DISCUSSION

Pex19p has been cloned and characterized from two different yeasts (*P. pastoris* and *S. cerevisiae*), mammalian cells (Chinese hamster and human PxF), and homologous ORFs identified in *C. elegans* and *S. pombe*. We identified the *P. pastoris* *PEX19* gene, characterized the mutant cells, analyzed the protein product, and defined protein-protein interactions. These results combined with information regarding Pex19p from other systems reinforce the convergence of model systems used to study peroxisomes. Despite the fact that the overall identity between the various Pex19p orthologues is low, several lines of evidence suggest that they belong to the same Pex group. First, all six proteins are approximately the same size, are hydrophilic, and contain a consensus sequence for farnesylation at the carboxyl terminus. In addition, there are regions of homology that are conserved between all the ortho-

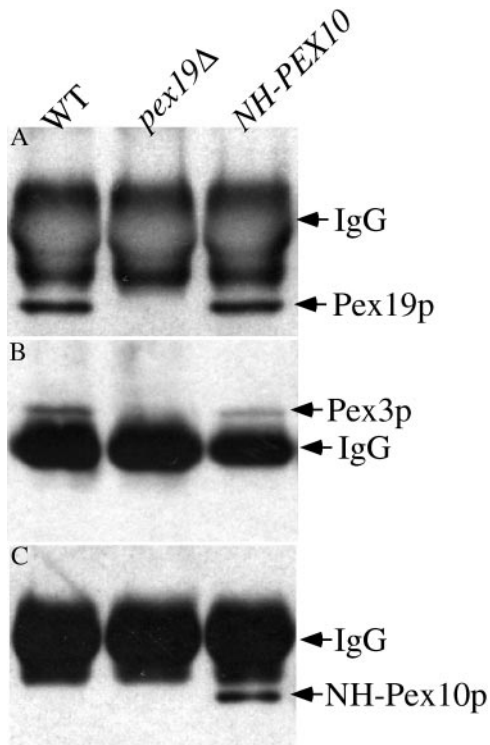


Figure 12. Coimmunoprecipitation of Pex3p and NH-Pex10p with Pex19p. Pex19p was immunoprecipitated from cleared lysates of wild-type (SMD1163), *pex19Δ* (SKF14), or *NH-PEX10* (SSH18) strains as described in MATERIALS AND METHODS. The material was resolved by SDS-PAGE and analyzed by immunoblotting with anti-Pex19p (A), anti-Pex3p (B), and anti-NH antibodies (C).

logues, and these regions are scattered throughout the proteins (Figure 1). Finally, similar protein-protein interactions have been observed for Pex19p from *S. cerevisiae* and *P. pastoris*.

Novel Peroxisome Remnants in *pex19Δ* Cells

Previous studies in *S. cerevisiae* had suggested that the *pex19Δ* strain lacks peroxisome remnants (Götte *et al.*, 1998). This conclusion was based solely on observations using electron microscopy. However, our immunofluorescence studies (Figures 5 and 6), particularly with the greater resolution afforded by the deconvolution microscope (Figure 6), and the biochemical fractionation experiments (Figure 4, B and C) show unequivocally the presence of small spherical and tubular remnants containing Pex3p in the *pex19Δ* strain. It is noteworthy that these remnants could easily have been missed using conventional immunofluorescence or electron microscopy, because the structures are much smaller and morphologically distinct from the remnants observed in many other *pex* mutants or the large (~1.3- μ m-diameter) cluster of peroxisomes seen in wild-type cells (Figure 5). Consistent

with earlier reports, no normal peroxisomes, or the usual peroxisome remnant structures observed in many other *pex* mutants (Gould *et al.*, 1992, 1996; McCollum *et al.*, 1993; Spong and Subramani, 1993; Heyman *et al.*, 1994; Kalish *et al.*, 1995, 1996; Liu *et al.*, 1995; Waterham *et al.*, 1996; Elgersma *et al.*, 1998), were seen in *Pppex19Δ* cells by electron microscopy. However, structures resembling the spherical and tubular forms seen by deconvolution microscopy were observed in our electron micrographs (Figure 7C). It is quite possible that these unusual remnants were missed in *S. cerevisiae* because they represent novel structures not observed in other *pex* mutants. Others have also stressed the importance of immunofluorescence for the identification of remnants in mutants when they were not observed by electron microscopy (Purdue and Lazarow, 1995). In addition, when the *pex19Δ* allele was introduced into *pex* mutant strains that contained the normal, large peroxisome remnants, these double mutants contained only the type of remnants seen in *pex19Δ* mutants (Snyder, unpublished observation), suggesting that the *pex19Δ* remnants are formed before the remnants seen in other *pex* mutants (see below).

Farnesylation of PpPex19p Is Not Essential for Peroxisome Biogenesis

Despite the finding that the Chinese hamster, human, and *S. cerevisiae* Pex19/PxF proteins are modified by farnesylation at a conserved CaaX motif (James *et al.*, 1994; Kammerer *et al.*, 1997; Götte *et al.*, 1998), this modification is unnecessary for PpPex19p function. ScPex19p migrates as a doublet in SDS-PAGE; the faster-migrating species is the farnesylated form, which comprises ~60% of the steady-state level of Pex19p (Götte *et al.*, 1998). We only detect a single band of Pex19p in *P. pastoris* (Figures 8A and 9C), suggesting that this modification is absent under the induction conditions tested, despite the fact that the carboxyl-terminal sequence CKQQ, which is farnesylated in *S. cerevisiae*, is fully conserved in PpPex19p. Furthermore, PpPex19p mutant proteins that cannot be modified by farnesylation, Pex19pC296ter and Pex19pC296S, fully complement *Pppex19Δ* mutant cells for growth on methanol or oleate (Figure 9A) and contain morphologically wild-type peroxisomes that import catalase (Figure 9B). In addition, the point mutant has the same mobility in SDS-PAGE as the wild-type protein (Figure 9C). These observations contrast results obtained for ScPex19p, for which farnesylation is clearly involved in protein function. What purpose the farnesylation serves in *S. cerevisiae* and how this requirement is bypassed in *P. pastoris* remain to be determined. Taken together, these data strongly suggest that PpPex19p is not farnesylated; however, we cannot rule out the possibility that farnesylation

may be transient or occur at a different time of peroxisome induction other than the ones tested here.

Other observations also raise questions about the functional significance of farnesylation of Pex19p: 1) in *S. cerevisiae*, not all of the protein is modified, suggesting that modification is slow, or perhaps reversible; 2) the addition of a hydrophobic molecule such as farnesyl might be expected to act as a membrane anchor, but the majority of yeast Pex19p has been localized to the cytosol; and 3) in *S. cerevisiae* the Pex19pC347S allows partial complementation of *pex19Δ* cells, suggesting that farnesylation is not an absolute requirement for ScPex19p function. Farnesylation seems only to improve the efficiency of Pex19p function in *S. cerevisiae* and may be redundant in *P. pastoris*, either because of the extended carboxyl terminus of the PpPex19p relative to the other orthologues or some other activity.

The Subcellular Localization of Pex19p

Pex19p was found predominantly in the cytosolic fractions of *P. pastoris* (Figure 8B), *S. cerevisiae* (Götte *et al.*, 1998), and Chinese hamster (James *et al.*, 1994) cells. However, the mammalian orthologues and overexpressed myc-ScPex19p have been observed at the peroxisome membrane by electron microscopy (James *et al.*, 1994; Kammerer *et al.*, 1997; Götte *et al.*, 1998). Perhaps the protein is loosely associated with peroxisomes, and this association is disrupted by biochemical manipulations. Moreover, a small fraction of total cellular Pex19p that associates with the peroxisome may be detected immunocytochemically, because of the high local concentration, but the majority of the protein could essentially go unnoticed in the cytosol because of low local concentrations. For now we must conclude that the majority of PpPex19p resides in a nonperoxisomal, cytosolic location, and that a small pool may transiently associate with peroxisomes, perhaps by binding to Pex3p (see below).

Interactions of Pex19p with Other Peroxins

We demonstrate that PpPex19p interacts with two PMPs, Pex3p and Pex10p (Figures 10–12). ScPex19p interacts with the ScPex3p (Götte *et al.*, 1998), and our results confirm this interaction in *P. pastoris*. In addition, we show that the extreme amino terminus (amino acids 1–42) of PpPex19p interacts with the carboxyl-terminal domain (110–455) of Pex3p. PpPex3p contains a putative transmembrane domain at amino acids 149–174, suggesting that the carboxyl-terminal two-thirds of the protein are on one side of the peroxisomal membrane. Indeed, protease protection experiments suggest that the majority of the protein, and thus this carboxyl-terminal region of PpPex3p, is exposed to the cytosol (our unpublished data). This topology of PpPex3p is consistent with that reported for

ScPex3p (Höhfeld *et al.*, 1991). This result allows us to conclude that the cytosolic domain of Pex3p interacts with Pex19p. Consistent with these observations is the hypothesis that Pex19p, which is predominantly cytosolic, transiently interacts with the cytosolic domain of Pex3p, which acts like a Pex19p receptor (Götte *et al.*, 1998). The minor amount of Pex19p found in the organelle pellet fraction might represent the pool that is transiently interacting with Pex3p at the peroxisome. The apparent instability of Pex3p in oleate-grown *pex19Δ* cells (Figure 3A) could be caused by its missing binding partner, Pex19p.

Interaction of the extreme carboxyl terminus of Pex19p with Pex10p suggests that Pex19p might have multiple functions. Because much of Pex10p, including its zinc-binding domain, is believed to be within the peroxisome lumen (Kalish *et al.*, 1995), Pex19p likely interacts with Pex10p before its insertion in the membrane. In this regard, Pex19p may function to facilitate the targeting, import, or assembly of Pex10p at the peroxisome. On the other hand, Pex19p may interact with the small cytosolic domain of Pex10p (amino acids 193–217). We must point out that the topology model for human Pex10p (Warren *et al.*, 1998) is opposite from that of PpPex10p; therefore caution must be used when incorporating the topology data into interaction models. Nonetheless, we believe that the interactions of Pex19p with the two PMPs must be transient, because the majority of Pex19p is not found on the peroxisome membrane. Additional studies will be required to determine the functional significance of the interaction of Pex19p with Pex3p and Pex10p.

Role of Pex19p in Peroxisome Biogenesis

A role for Pex19p in peroxisome biogenesis and the import of peroxisomal proteins has been clearly established for *P. pastoris* and *S. cerevisiae*. In both yeast mutants there is a strong defect for the import of both PTS1- and PTS2-containing peroxisomal matrix proteins. Because *Pppex19Δ* cells clearly contain novel peroxisome remnants that are smaller and morphologically distinct (termed early remnants) from those (late remnants) seen in most other *pex* mutants, we postulate that the structures accumulating in the absence of Pex19p are normal intermediates (and not aberrant structures) in peroxisome biogenesis. If this is true, we propose the following model for peroxisome biogenesis. Early remnants that accumulate in the *pex19Δ* strain progress by further protein and/or membrane addition to the late remnants seen in other *pex* mutants, and these, in turn, mature to normal peroxisomes by the import of matrix proteins. In this model, Pex19p has a direct role in the maturation of the early remnants to the late ones. We do not know whether the block in the *pex19Δ* strain is due to the inability to

incorporate certain PMPs into the peroxisomal membrane or due to some other defect, such as lipid addition. However, because Pex3p is found in the early remnant, its incorporation into membranes could not be dependent on Pex19p. Rather, Pex3p may serve as the Pex19p receptor to transiently dock it at the peroxisome membrane. This would be consistent with the hypothesis that for the earliest stages of peroxisome biogenesis Pex3p functions concurrently with Pex19p. This notion is also supported by previous reports that *pex3Δ* cells have no remnants, although those results have to be reexamined in the light of the novel remnants reported here in the *pex19Δ* strain (Höhfeld *et al.*, 1991; Baerends *et al.*, 1996; Wiemer *et al.*, 1996).

The functional significance of the Pex19p–Pex10p interaction is likely different from the Pex3p–Pex19p interaction. *pex10* mutant cells contain late remnant membranes (Kalish *et al.*, 1995), suggesting that Pex19p performs early functions, proposed above, that are epistatic to a later Pex10p function. One possibility is that the Pex19p–Pex10p interaction is necessary for the import and/or assembly of Pex10p into peroxisomes and that Pex10p has to be in the early remnants for them to mature into normal peroxisomes.

An alternative to the biogenesis model presented above is the possibility that Pex19p coordinates growth and division of peroxisomes, and in its absence these are no longer coordinated, leading to the development of small membrane fragments by unchecked division. Growth and division of peroxisomes must be tightly controlled to maintain the normal size and morphology of the organelle in wild-type cells. In *pex19Δ* cells, the Pex3p-containing structures might be created by the inability to maintain a large organelle, not due to a defect in maturation from a preperoxisome to a peroxisome as suggested above. The fragmentation would be due to unregulated division in the absence of coordinated growth. This is consistent with the conclusion from *Hansenula polymorpha* studies that Pex3p is required for the maintenance of the peroxisome membrane (Baerends *et al.*, 1996) and our hypothesis that Pex19p may function concurrently during this process. Additional support for a role of Pex10p in this process is again provided from *H. polymorpha* experiments, which suggest that Pex10p functions to regulate peroxisome division (Tan *et al.*, 1995). With these observations in mind, it would be reasonable to suggest that the interacting proteins Pex19p, Pex3p, and Pex10p function to regulate peroxisome division. In this scenario, Pex19p and Pex3p would act like negative regulators of division, whereas Pex10p would perform a stimulatory role.

Future experiments will be required to address what, if any, remnant structures containing peroxisomal markers exist in the *pex3Δ* mutants and whether other PMPs localize to the same structures in *pex3Δ*

and *pex19Δ* cells. Clearly we must distinguish between the possibilities that Pex19p mediates recruitment of membrane from an as yet unidentified source, or the fusion of early remnants into larger structures, and the assembly of membrane components to allow luminal import to begin. In addition, it will be important to determine whether these types of remnant structures are a normal precursor in the biosynthesis of peroxisomes or the product of aberrant peroxisome division. Isolation of conditional alleles of *PEX19* could help distinguish these possibilities.

The origin of the early remnants is an intriguing question that is relevant in light of recent suggestions that ER-derived vesicles play a role in peroxisome biogenesis (Titorenko and Rachubinski, 1998). It will also be interesting to determine the connection between the nonperoxisomal membranous structures containing the two AAA-ATPases, Pex1p and Pex6p (Faber *et al.*, 1998), and the types of remnants described here.

ACKNOWLEDGMENTS

We thank Jim Cregg for providing strains and unpublished information about *pex* mutant collections and Su Hua for technical assistance. We are grateful to Kit Pogliano and Joe Pogliano for assistance with the deconvolution microscopy and Scott Emr for use of his microscope. We also appreciate the advice of Peter Rehling, Andy Wurmser, and Marcus Babst. This work was supported by fellowships from the American Cancer Society (to W.B.S.), the Human Frontier Science Program Organization (to K.N.F.), the European Molecular Biology Organization (to T.J.W.), the Swiss National Funds (to A.K.), and the Deutsche Forschungsgemeinschaft (to G.H.L.) and National Institutes of Health grant NIHDK-41737 and the March of Dimes (to S.S.). The nucleotide sequence of *PpPEX19* has been submitted to GenBank with accession number AF133271.

REFERENCES

- Babst, M., Sato, T.K., Banta, L.M., and Emr, S.D. (1997). Endosomal transport function in yeast requires a novel AAA-type ATPase, Vps4p. *EMBO J.* 16, 1820–1831.
- Babst, M., Wendland, B., Estepa, E.J., and Emr, S.D. (1998). The Vps4p AAA ATPase regulates membrane association of a Vps protein complex required for normal endosome function. *EMBO J.* 17, 2982–2993.
- Baerends, R.J.S., Rasmussen, S.W., Hilbrands, R.E., van der Heide, M., Faber, K.N., Reuvekamp, P.T.W., Kiel, J.A.K.W., Cregg, J.M., van der Klei, I., and Veenhuis, M. (1996). The *Hansenula polymorpha* *PER9* gene encodes a peroxisomal membrane protein essential for peroxisome assembly and integrity. *J. Biol. Chem.* 271, 8887–8894.
- Braun, A., Kammerer, S., Weissenhorn, W., Weiss, E.H., and Cleve, H. (1994). Sequence of a putative human housekeeping gene (HK33) localized on chromosome 1. *Gene* 146, 291–295.
- De Duve, C. (1996). The peroxisome in retrospect. *Ann. NY Acad. Sci.* 804, 1–10.
- Distel, B., *et al.* (1996). A unified nomenclature for peroxisome biogenesis factors. *J. Cell Biol.* 135, 1–3.
- Elgersma, Y., Elgersma, H.M., Wenzel, T., McCaffery, J.M., Farquhar, M.G., and Subramani, S. (1998). A mobile PTS2 receptor for

- peroxisomal protein import in *Pichia pastoris*. *J. Cell Biol.* *140*, 807–820.
- Elgersma, Y., Kwast, L., van den Berg, M., Snyder, W.B., Distel, B., Subramani, S., and Tabak, H.F. (1997). Overexpression of Pex15p, a phosphorylated peroxisomal integral membrane protein required for peroxisome assembly in *S. cerevisiae*, causes proliferation of the endoplasmic reticulum membrane. *EMBO J.* *16*, 7326–7341.
- Elgersma, Y., Van den Berg, M., Tabak, H.F., and Distel, B. (1993). An efficient positive selection procedure for the isolation of peroxisomal import and peroxisome assembly mutants of *Saccharomyces cerevisiae*. *Genetics* *135*, 731–740.
- Elgersma, Y., Vos, A., van den Berg, M., van Roermund, C.W., van der Sluijs, P., Distel, B., and Tabak, H.F. (1996). Analysis of the carboxyl-terminal peroxisomal targeting signal 1 in a homologous context in *Saccharomyces cerevisiae*. *J. Biol. Chem.* *271*, 26375–26382.
- Ellis, S.B., Brust, P.F., Koutz, P.J., Waters, A.F., Harpold, M.M., and Gingeras, T.R. (1985). Isolation of alcohol oxidase and two other methanol regulatable genes from the yeast *Pichia pastoris*. *Mol. Cell. Biol.* *5*, 1111–1121.
- Faber, K.N., Heyman, J.A., and Subramani, S. (1998). Two AAA family peroxins, PpPex1p and PpPex6p, interact with each other in an ATP-dependent manner and are associated with different subcellular membranous structures distinct from peroxisomes. *Mol. Cell. Biol.* *18*, 936–943.
- Fransen, M., Terlecky, S.R., and Subramani, S. (1998). Identification of a human PTS1 receptor docking protein directly required for peroxisomal protein import. *Proc. Natl. Acad. Sci. USA* *95*, 8087–8092.
- Götte, K., Girzalsky, W., Linkert, M., Baumgart, E., Kammerer, S., Kunau, W.H., and Erdmann, R. (1998). Pex19p, a farnesylated protein essential for peroxisome biogenesis. *Mol. Cell. Biol.* *18*, 616–628.
- Gould, S.J., Kalish, J.E., Morrell, J.C., Bjorkman, J., Urquhart, A.J., and Crane, D.I. (1996). Pex13p is an SH3 protein of the peroxisome membrane and a docking factor for the predominantly cytoplasmic PTS1 receptor. *J. Cell Biol.* *135*, 85–95.
- Gould, S.J., Keller, G.-A., Hosken, N., Wilkinson, J., and Subramani, S. (1989). A conserved tripeptide sorts proteins to peroxisomes. *J. Cell Biol.* *108*, 1657–1664.
- Gould, S.J., Keller, G.-A., and Subramani, S. (1987). Identification of a peroxisomal targeting signal at the carboxy terminus of firefly luciferase. *J. Cell Biol.* *105*, 2923–2931.
- Gould, S.J., McCollum, D., Spong, A.P., Heyman, J.A., and Subramani, S. (1992). Development of the yeast *Pichia pastoris* as a model organism for a genetic and molecular analysis of peroxisome assembly. *Yeast* *8*, 613–628.
- Hajra, A.K., and Bishop, J.E. (1982). Glycerolipid biosynthesis in peroxisomes via the acyl dihydroxyacetone phosphate pathway. *Ann. NY Acad. Sci.* *386*, 170–182.
- Heyman, J.A., Monosov, E., and Subramani, S. (1994). Role of the *PAS1* gene of *Pichia pastoris* in peroxisome biogenesis. *J. Cell Biol.* *127*, 1259–1273.
- Höfheld, J., Veenhuis, M., and Kunau, W.H. (1991). *PAS3*, a *Saccharomyces cerevisiae* gene encoding a peroxisomal integral membrane protein essential for peroxisome biogenesis. *J. Cell Biol.* *114*, 1167–1178.
- Huhse, B., Rehling, P., Albertini, M., Blank, L., Meller, K., and Kunau, W.H. (1998). Pex17p of *Saccharomyces cerevisiae* is a novel peroxin and component of the peroxisomal protein translocation machinery. *J. Cell Biol.* *140*, 49–60.
- James, G.L., Goldstein, J.L., Pathak, R.K., Anderson, R.G., and Brown, M.S. (1994). PxF, a prenylated protein of peroxisomes. *J. Biol. Chem.* *269*, 14182–14190.
- Kalish, J.E., Keller, G.A., Morrell, J.C., Mihalik, S.J., Smith, B., Cregg, J.M., and Gould, S.J. (1996). Characterization of a novel component of the peroxisomal protein import apparatus using fluorescent peroxisomal proteins. *EMBO J.* *15*, 3275–3285.
- Kalish, J.E., Theda, C., Morrell, J.C., Berg, J.M., and Gould, S.J. (1995). Formation of the peroxisome lumen is abolished by loss of *Pichia pastoris* Pas7p, a zinc-binding integral membrane protein of the peroxisome. *Mol. Cell. Biol.* *15*, 6406–6419.
- Kammerer, S., Arnold, N., Gutensohn, W., Mewes, H.W., Kunau, W.H., Hofler, G., Roscher, A.A., and Braun, A. (1997). Genomic organization and molecular characterization of a gene encoding HsPXF, a human peroxisomal farnesylated protein. *Genomics* *45*, 200–210.
- Laemmli, U.K. (1970). Cleavage of structural proteins during the assembly of the head of bacteriophage T4. *Nature* *227*, 680–685.
- Lazarow, P.B., and De Duve, C. (1976). A fatty acyl-CoA oxidizing system in rat liver peroxisomes; enhancement by clofibrate, a hypolipidemic drug. *Proc. Natl. Acad. Sci. USA* *73*, 2043–2046.
- Lazarow, P.B., and Fujiki, Y. (1985). Biogenesis of peroxisomes. *Annu. Rev. Cell Biol.* *1*, 489–530.
- Lazarow, P.B., and Moser, H.W. (1989). Disorders of peroxisome biogenesis. In: *The Metabolic Basis of Inherited Disease*, ed. C.R. Scriver, A.L. Beaudet, W.S. Sly, and D. Valle, New York: McGraw-Hill, 1479–1509.
- Liu, H., Tan, X., Russell, K.A., Veenhuis, M., and Cregg, J.M. (1995). PER3, a gene required for peroxisome biogenesis in *Pichia pastoris*, encodes a peroxisomal membrane protein involved in protein import. *J. Biol. Chem.* *270*, 10940–10951.
- McCollum, D., Monosov, E., and Subramani, S. (1993). The *pas8* mutant of *Pichia pastoris* exhibits the peroxisomal protein import deficiencies of Zellweger syndrome cells—the *PAS8* protein binds to the COOH-terminal tripeptide peroxisomal targeting signal, and is a member of the TPR protein family. *J. Cell Biol.* *121*, 761–774.
- Monosov, E.Z., Wenzel, T.J., Luers, G.H., Heyman, J.A., and Subramani, S. (1996). Labeling of peroxisomes with green fluorescent protein in living *P. pastoris* cells. *J. Histochem. Cytochem.* *44*, 581–589.
- Odorizzi, G., Babst, M., and Emr, S.D. (1998). Fab1p PtdIns(3)P 5-kinase function essential for protein sorting in the multivesicular body. *Cell* *95*, 847–858.
- Osumi, T., Tsukamoto, T., Hata, S., Yokota, S., Miura, S., Fujiki, Y., Hijikata, M., Miyazawa, S., and Hashimoto, T. (1991). Amino-terminal presequence of the precursor of peroxisomal 3-ketoacyl-CoA thiolase is a cleavable signal peptide for peroxisomal targeting. *Biochem. Biophys. Res. Commun.* *181*, 947–954.
- Pogliano, J., Osborne, N., Sharp, M.D., Abanes-De Mello, A., Perez, A., Sun, Y.-L., and Pogliano, K. (1999). A vital stain for studying membrane dynamics in bacteria: a novel mechanism controlling septation during *Bacillus subtilis* sporulation. *Mol. Microbiol.* *31*, 1149–1159.
- Purdue, P.E., and Lazarow, P.B. (1995). Identification of peroxisomal membrane ghosts with an epitope-tagged integral membrane protein in yeast mutants lacking peroxisomes. *Yeast* *11*, 1045–1060.
- Purdue, P.E., Yang, X., and Lazarow, P.B. (1998). Pex18p and Pex21p, a novel pair of peroxins essential for peroxisomal targeting by the PTS2 pathway. *J. Cell Biol.* *143*, 1859–1869.
- Rehling, P., Albertini, M., and Kunau, W.H. (1996). Protein import into peroxisomes: new developments. *Ann. NY Acad. Sci.* *804*, 34–46.

- Sakai, Y., Koller, A., Rangell, L.K., Keller, G.A., and Subramani, S. (1998). Peroxisome degradation by microautophagy in *Pichia pastoris*: identification of specific steps and morphological intermediates. *J. Cell Biol.* *141*, 625–636.
- Sambrook, J., Fritsch, E.F., and Maniatis, T. (1989). *Molecular Cloning: A Laboratory Manual*, Cold Spring Harbor, NY: Cold Spring Harbor Laboratory Press.
- Sanger, F., Nicklen, S., and Coulson, A.R. (1977). DNA sequencing with chain-terminating inhibitors. *Proc. Natl. Acad. Sci. USA* *74*, 5463–5467.
- Sears, I.B., O'Connor, J., Rossanese, O.W., and Glick, B.S. (1998). A versatile set of vectors for constitutive and regulated gene expression in *Pichia pastoris*. *Yeast* *14*, 783–790.
- Spong, A.P., and Subramani, S. (1993). Cloning and characterization of *PAS5*: a gene required for peroxisome biogenesis in the methylotrophic yeast *Pichia pastoris*. *J. Cell Biol.* *123*, 535–548.
- Stack, J.H., Herman, P.K., Schu, P.V., and Emr, S.D. (1993). A membrane-associated complex containing the Vps15 protein kinase and the Vps34 PI 3-kinase is essential for protein sorting to the yeast lysosome-like vacuole. *EMBO J.* *12*, 2195–2204.
- Subramani, S. (1997). *PEX* genes on the rise. *Nat. Genet.* *15*, 331–333.
- Subramani, S. (1998). Components involved in peroxisome import, biogenesis, proliferation, turnover, and movement. *Physiol. Rev.* *78*, 171–188.
- Swinkels, B.W., Gould, S.J., Bodnar, A.G., Rachubinski, R.A., and Subramani, S. (1991). A novel, cleavable peroxisomal targeting signal at the amino-terminus of the rat 3-ketoacyl-CoA thiolase. *EMBO J.* *10*, 3255–3262.
- Tan, X., Waterham, H.R., Veenhuis, M., and Cregg, J.M. (1995). The *Hansenula polymorpha* *PER8* gene encodes a novel peroxisomal integral membrane protein involved in proliferation. *J. Cell Biol.* *128*, 307–319.
- Thompson, S.L., and Krisans, S.K. (1990). Rat liver peroxisomes catalyze the initial step in cholesterol synthesis. The condensation of acetyl-CoA units into acetoacetyl-CoA. *J. Biol. Chem.* *265*, 5731–5735.
- Titorenko, V.I., and Rachubinski, R.A. (1998). The endoplasmic reticulum plays an essential role in peroxisome biogenesis. *Trends Biochem. Sci.* *23*, 231–233.
- Titorenko, V.I., Smith, J.J., Szilard, R.K., and Rachubinski, R.A. (1998). Pex20p of the yeast *Yarrowia lipolytica* is required for the oligomerization of thiolase in the cytosol and for its targeting to the peroxisome. *J. Cell Biol.* *142*, 403–420.
- Tolbert, N.E., and Essner, E. (1981). Microbodies: peroxisomes and glyoxysomes. *J. Cell Biol.* *91*, 271s–283s.
- Towbin, H., Staehelin, T., and Gordon, J. (1979). Electrophoretic transfer of proteins from polyacrylamide gels to nitrocellulose sheets: procedure and some applications. *Proc. Natl. Acad. Sci. USA* *76*, 4350–4354.
- Veenhuis, M.J., Keizer, I., and Harder, W. (1979). Characterization of peroxisomes in glucose-grown *Hansenula polymorpha* and their development after the transfer of cells into methanol-containing media. *Arch. Microbiol.* *120*, 167–175.
- Warren, D.S., Morrell, J.C., Moser, H.W., Valle, D., and Gould, S.J. (1998). Identification of PEX10, the gene defective in complementation group 7 of the peroxisome-biogenesis disorders. *Am. J. Hum. Genet.* *63*, 347–359.
- Waterham, H.R., de Vries, Y., Russel, K.A., Xie, W., Veenhuis, M., and Cregg, J.M. (1996). The *Pichia pastoris* *PER6* gene product is a peroxisomal integral membrane protein essential for peroxisome biogenesis and has sequence similarity to the Zellweger syndrome protein PAF-1. *Mol. Cell Biol.* *16*, 2527–2536.
- Wiemer, E.A.C., Luers, G., Faber, K.N., Wenzel, T., Veenhuis, M., and Subramani, S. (1996). Isolation and characterization of Pas2p, a peroxisomal membrane protein essential for peroxisome biogenesis in the methylotrophic yeast *Pichia pastoris*. *J. Biol. Chem.* *271*, 18973–18980.